

Processing Classical Holographic Interferograms by Algorithms of Digital Hologram Reconstruction

A. V. Belashov^{a, b}, N. V. Petrov^b, and I. V. Semenova^{a*}

^a Ioffe Institute, St. Petersburg, 194021 Russia

^b St. Petersburg National Research University of Information Technologies, Mechanics and Optics, St. Petersburg, 197101 Russia

*e-mail: Irina.Semenova@mail.ioffe.ru

Received November 21, 2014

Abstract—The capability of digital hologram reconstruction algorithms applied for the processing of holographic interferograms in finite-width fringes being recorded and reconstructed by the classical optical method is validated. Application of these algorithms, significantly simplifies the processing procedure. Results of the processing of the holographic interferogram of a bulk strain soliton performed by the two methods are demonstrated to be in a good agreement.

DOI: 10.1134/S1063785015070184

The rapid development of digital data recording technologies has led to wide use of digital holography techniques [1, 2]. However, these techniques still have some limitations, which are related primarily to insufficient spatial resolution and recording speed of presently available digital cameras. While the problem of restricted resolution can be readily solved by using a standard commercial scanner in the recording system [3], the high frame rate required for studies of fast processes leads to the need for special high-speed cameras [4, 5]. Alternatively, it is possible to use methods of classical holographic interferometry that employ recording on photographic materials followed by optical data reconstruction.

The method of classical double exposure holographic interferometry is based on the sequential recording of two holograms of an object in two states at the same place on a high-resolution recording medium. In the method of finite-width fringes, the angle between the object and reference beams is slightly varied, e.g., by rotating a wedge in the object beam. At the stage of reconstruction, this leads to the appearance of carrier fringes, which deviations from straight lines are related to a phase difference caused by the object disturbance, whereby the shift by the carrier fringe width ($\Delta K = 1$) corresponds to a phase variation of 2π .

Imperfections of the optical system and disturbances introduced by the object under study frequently lead to the appearance of various defects on the interferogram, primarily in the form of carrier fringe discontinuities. The presence of such defects significantly complicates implementation of the automatic tracing of a carrier fringe and the measurement

of its deviation using well-known processing algorithms.

The present work was aimed at developing a reliable and relatively simple method for the automatic processing of classical holographic interferograms. It is demonstrated below that this task can be solved using existing algorithms that are well developed for reconstructing off-axis digital holograms.

As is known, a holographic interferogram in finite-width fringes represents a result of the interference of two object waves with phase components φ_1 and φ_2 at a certain angle that adds flat inclined phase γ to one of the object waves. The difference of phase distributions $\varepsilon = \varphi_1 - \varphi_2$ corresponds to changes appearing in the object between the two exposures. The interference of two object waves, $A \exp(i\varphi_1)$ and $B \exp(i(\varphi_2 + \gamma))$, is described by the following equation:

$$I = |A \exp(i\varphi_1) + B \exp(i(\varphi_2 + \gamma))|^2 \quad (1) \\ = A^2 + B^2 + 2AB \cos(\varphi_1 - (\varphi_2 + \gamma)),$$

where $\cos(\varphi_1 - (\varphi_2 + \gamma))$ is the interference term. However, the same interference pattern can alternatively be interpreted by considering it as a hologram obtained as a result of the interaction of an object wave, having the phase ε of disturbance of the object under study, and a plane reference wave with the phase γ_0 at angle θ between the two waves. In this case, the interference term is also described by the expression $\cos(\varepsilon - \gamma_0) = \cos(\varphi_1 - \varphi_2 - \gamma_0)$.

This assumption was verified by numerically simulating the pattern of interference at angle θ for two object waves corresponding to the presence (Fig. 1a) and absence (Fig. 1b) of disturbance and comparing it to the digital hologram obtained with the object wave

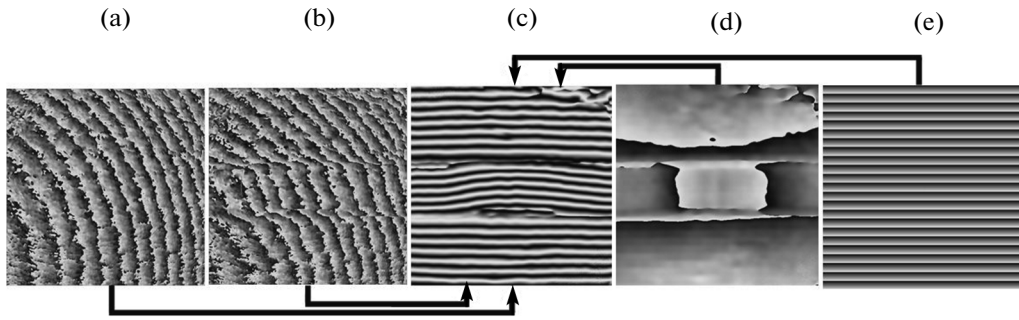


Fig. 1. Results of simulation of the formation of the holographic interferogram (a–c) and of the off-axis digital holograms (c–e).

bearing information on the object disturbance (Fig. 1d) and the reference wave inclined by angle θ (Fig. 1e). As can be seen, these approaches lead to the same distribution of intensity (Fig. 1c)

Then, by applying the known algorithm of reconstruction of the off-axis digital hologram to the

obtained interferogram and assuming the angle between object and reference waves to be θ , one can readily obtain the array of phase retardation values caused by changes in the object under study. This angle can be either measured in experiment or calculated based on the parameters of interference fringes in the

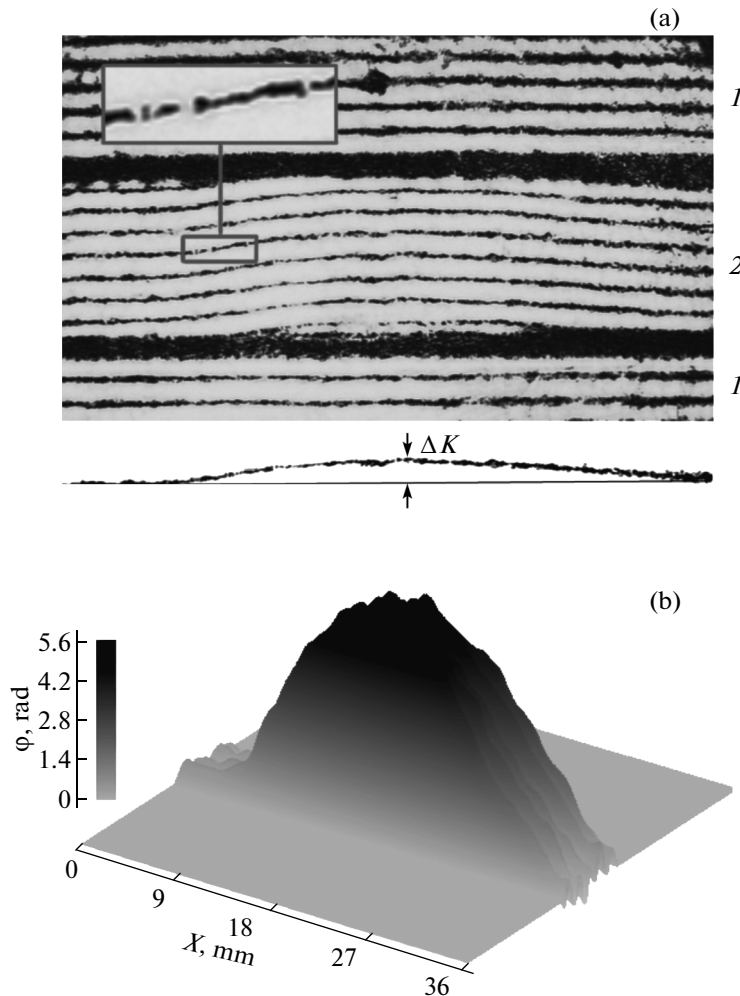


Fig. 2. (a) Holographic interferogram of a bulk strain soliton in homogeneous PS waveguide (2) in surrounding air (1) (the shape of one interference fringe with shift ΔK is shown below the interferogram) and (b) result of interferogram processing by the digital hologram reconstruction algorithm [7].

undisturbed region [6]. Thus, the difference between classical holographic interferometry and the off-axis digital holography reduces essentially to regrouping phase components in the interference term. This is equivalent to interchanging the notation of reference and object waves.

A number of algorithms are developed by now aimed for reconstruction of off-axis digital holograms. However, in view of the rather large number of carrier fringe discontinuities in the case under consideration (for example, see the inset in Fig. 2a), it is effective to employ an algorithm that is stable to such defects. From this standpoint, significant advantages are offered by the local least-squares algorithm of phase reconstruction proposed by Liebling et al. [7]. This algorithm is based on the assumption that amplitudes of the object and reference waves as well as the object wave phase vary much more slowly than the phase of a plane reference wave and the recorded intensity do. This assumption is valid in the overwhelming number of cases because the reference wave is incident onto the recording medium at a certain angle rather than perpendicularly and its phase front can be readily modeled using a priori information about the angle θ . Then, each pixel is considered being surrounded by a small square region of $N \times N$ pixels, in which slowly varying parameters are assumed to be constant, and a system of $M = N^2$ overdetermined equations is constructed with three unknowns: amplitudes of the object and reference waves and the object wave phase. Finally, the unknown values are determined by solving the obtained system of equations. The assumption of a slowly varying phase of the object wave provides a rather smooth distribution of phase shift even in the presence of a large number of small discontinuities of carrier fringes. The degree of smoothing is determined by the size of the local region in which the system of overdetermined equations is constructed [8].

The above algorithm has been applied to the processing of holographic interferograms of a bulk strain soliton in a homogeneous polystyrene (PS) waveguide. The initial interferogram is presented in Fig. 2a. In the classical case, such holographic interferograms are processed by measuring interference fringe shifts. In the example provided, we used the algorithm of [7] and obtained an array of phase retardations (Fig. 2b). As can be seen, the shape of the curve circumscribing the phase variation array matches at of the carrier fringe on the interferogram recorded by the method of double exposure holographic interferometry, while the processed image (Fig. 2b) does not exhibit discontinuities or other singularities present on the interferogram.

The amplitude of the observed bulk strain soliton can be calculated from the carrier fringe shifts by the following formula [9]:

$$A = \frac{\Delta K \lambda}{h(n_1 - 1)(1 - \nu)}, \quad (2)$$

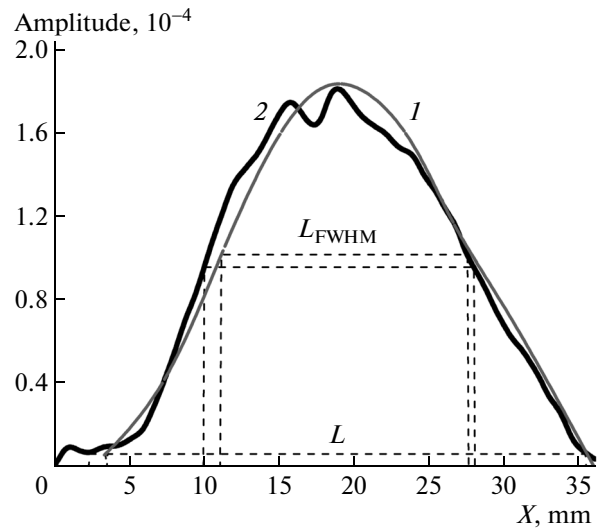


Fig. 3. The shape of a bulk strain soliton in homogeneous PS waveguide as obtained by processing of the holographic interferogram (presented in Fig. 2a) using (1) the classical method (curve constructed using seven points and smoothed by β spline) and (2) the digital hologram reconstruction algorithm [7]. Dashed lines show the soliton width (L) and full width at half maximum (L_{FWHM}).

where ΔK is the carrier fringe shift on the interferogram, λ is the recording radiation wavelength (0.694 μm), n_1 is the refractive index of waveguide material ($n_1 = 1.54$ for PS), h is the waveguide thickness (10 mm) in the direction of probing radiation, and ν is the Poisson's ratio ($\nu = 0.34$ for PS). Taking into account that $\Delta K = \varphi/2\pi$ (where φ is the phase), we eventually obtain the following formula:

$$A = \frac{\varphi \lambda}{2\pi h(n_1 - 1)(1 - \nu)}. \quad (3)$$

The results of processing of the interferogram presented in Fig. 2a gave maximum soliton amplitude $A_{\text{max}} = 1.82 \times 10^{-4}$, soliton width $L = 33.0$ mm, and full width at half maximum $L_{FWHM} = 17.8$ mm.

Figure 3 shows the shape of the bulk longitudinal strain soliton in the homogeneous PS waveguide as obtained by processing of the holographic interferogram (Fig. 2a) using the classical method (curve constructed by discrete seven points and smoothed by β spline) and the proposed algorithm applying the local least-squares wave retrieval procedure [7]. The discrepancy in soliton width L can be explained by a rather large error of determination of the fringe shift by the classical method for solitary waves with low-sloped fronts.

Thus, it has been demonstrated that the existing algorithms of digital hologram reconstruction can be applied to processing of holographic interferograms recorded and reconstructed by the classical optical method.

Acknowledgments. The financial support from the Russian Science Foundation under the grant no. 14-12-00342 is gratefully acknowledged. N. Petrov acknowledges support from the Ministry of Education and Science of the Russian Federation, project no. 2014/190.

REFERENCES

1. N. Verrier and M. Atlan, *Appl. Opt.* **50**, H136 (2011).
2. T. Tahara, Y. Awatsuji, Y. Shimozato, T. Kakue, K. Nishio, S. Ura, T. Kubota, and O. Matoba, *Opt. Lett.* **36**, 3254 (2011).
3. T. Shimobaba, H. Yamanashi, T. Kakue, M. Oikawa, N. Okada, Y. Endo, R. Hirayama, N. Masuda, and T. Ito, *Sci. Rep.* **3**, 2664 (2013).
4. M. Karray, C. Poilane, D. Mounier, M. Gargoury, and P. Picart, *Proc. SPIE* **8413**, 841311 (2012).
5. M. Leclercq, M. Karray, V. Isnard, F. Gautier, and P. Picart, *Appl. Opt.* **52**, A136 (2013).
6. A. V. Belashov, N. V. Petrov, I. V. Semenova, and O. S. Vasyutinskii, *J. Phys.: Conf. Ser.* **536**, 012003 (2014).
7. M. Liebling, T. Blu, and M. Unser, *J. Opt. Soc. Am. A* **21** (3), 367 (2004).
8. A. V. Belashov, N. V. Petrov, and I. V. Semenova, *Opt. Express* **22**, 28363 (2014).
9. G. V. Dreiden, K. R. Khusnutdinova, A. M. Samsonov, and I. V. Semenova, *Strain* **46** (6), 589 (2010).

Translated by P. Pozdeev